Characterization of the Inducible Nitric Oxide Synthase Oxygenase Domain Identifies a 49 Amino Acid Segment Required for Subunit Dimerization and Tetrahydrobiopterin Interaction†

Dipak K. Ghosh,‡,§ Chaoqun Wu,‡,§ Eva Pitters,∥ Michael Moloney,‡ Ernst R. Werner,⊥ Bernd Mayer,∥ and Dennis J. Stuehr*,‡

Department of Immunology, The Cleveland Clinic, Cleveland, Ohio 44195, Institut fur Pharmakologie und Toxicologie, Karl-Franzens-Universitat Graz, A-8010 Graz, Austria, and Insitut fur Medizinische Chemie und Biochemie, Universitat Innsbruck, A-6020 Innsbruck, Austria

Received January 30, 1997; Revised Manuscript Received July 9, 1997⊗

ABSTRACT: The oxygenase domain of inducible NO synthase (residues 1−498, iNOSox) is the enzyme's catalytic center. Its active form is a homodimer that contains heme and tetrahydrobiopterin (H4biopterin) and binds L-arginine [Ghosh, D. K., & Stuehr, D. J. (1995) *Biochemistry 34*, 801]. To help identify protein residues involved in prosthetic group and dimeric interaction, we expressed H4biopterin-free iNOSox in *Escherichia coli*. The iNOSox was 80% dimeric but contained a low-spin heme iron that bound DTT as a sixth ligand. The iNOSox bound H4biopterin or L-arginine with high affinity, which displaced DTT from the heme and caused spectral changes consistent with a closing up of the heme pocket. The H4biopterin-replete iNOSox could catalyze conversion of N^{ω}-hydroxyarginine to citrulline and NO in a H_2O_2-supported reaction. Limited trypsinolysis of the H4biopterin-free iNOSox dimer cut the protein at a single site in its N-terminal region (K117). H4biopterin protected against the cleavage whereas L-arginine did not. The resulting 40 kDa protein contained thiol-ligated low-spin heme, was monomeric, catalytically inactive, showed no capacity to bind H4biopterin or L-arginine, and did not dimerize when provided with these molecules, indicating that residues 1−117 were important for iNOSox dimerization and H4biopterin/L-arginine interaction. A deletion mutant missing residues 1−114 was partially dimeric but otherwise identical to the 40 kDa protein regarding its spectral and catalytic properties and inability to respond to L-arginine and H4biopterin, whereas a deletion mutant missing residues 1−65 was equivalent to wild-type iNOSox, narrowing the region of importance to amino acids 66−114. Mutation of a conserved cysteine in this region (C109A) decreased H4biopterin affinity without compromising iNOSox dimeric structure, L-arginine binding, or catalytic function. These results suggest that residues 66−114 of iNOSox are involved in productive H4biopterin interaction and subunit dimerization. H4biopterin binding appears to stabilize the protein structure in this region, and through doing so activates iNOS for NO synthesis.

The free radical nitric oxide (NO)[1] is an important effector molecule in the nervous, immune, and cardiovascular systems (Moncada et al, 1991; Bredt & Snyder, 1994; Nathan & Xie, 1994). NO is synthesized by three NO synthases (NOSs), all which catalyze an NADPH- and O_2-dependent oxidation of L-arginine to form citrulline and NO [for reviews see Griffith and Stuehr (1995) and Marletta (1993)]. Two NOS isoforms are constitutively expressed in cells such as neurons (nNOS) and endothelium (eNOS) and are activated by Ca^{2+}-dependent calmodulin (CaM) binding, whereas expression of a third isoform is cytokine induced. This latter isoform (iNOS) is continuously active due to its containing tightly bound CaM (Cho et al., 1992; Kroncke et al., 1995).

Despite differences in primary sequence, expression level, and regulation, all three NOSs are homodimeric enzymes whose subunits are comprised of an N-terminal oxygenase domain that binds iron protoporphyrin IX (heme), L-arginine, and tetrahydrobiopterin (H4biopterin) and a C-terminal reductase domain that binds calmodulin (CaM), FMN, FAD, and NADPH (Xie et al., 1992; Ghosh & Stuehr, 1995; Sheta et al., 1994; Bredt et al., 1991; Sessa et al., 1992). Each domain has distinct roles in catalysis and in forming and stabilizing the dimeric structure which is critical for enzyme activity (Ghosh & Stuehr, 1995; Sheta et al., 1994; Chen et al., 1996; McMillan & Masters, 1995; Abu-Soud et al., 1995). The reductase domain shuttles electrons from NADPH to the oxygenase domain, which is the site of heme iron reduction, oxygen activation, and NO synthesis [for reviews see Griffith and Stuehr (1995) and Marletta (1993)] . Studies with dimeric iNOS suggest that its subunits are aligned in a head-to-head manner, with the oxygenase domains participating in the dimeric interaction and the reductase domains

† This work was supported by National Institutes of Health Grants CA53914 (D.J.S.), P 10655, 10859, P11478 (B.M.), and P11301 (E.R.W.) from the Fonds zur Foerderung der Wissenshcaftlichen Forschung in Oesterreich. D.J.S. is an Established Investigator of the American Heart Association.

* Corresponding author. Tel: (216) 445-6950. Fax: (216) 444-9329. E.mail: stuehrd@cesmtp.ccf.org.

‡ The Cleveland Clinic.

§ These authors contributed equally to this work.

∥ Karl-Franzens-Universitat.

⊥ Universitat Innsbruck.

⊗ Abstract published in *Advance ACS Abstracts,* August 15, 1997.

[1] Abbreviations: BME, β-mercaptoethanol; CaM, calmodulin; EPPS, *N*-(2-hydroxyethyl)piperazine-*N*′-(3-propane sulfonic acid); IPTG, isopropyl thio-β-D-galactoside; iNOSox, inducible NO synthase oxygenase domain; NO, nitric oxide; NOHA, N^{ω}-hydroxy-L-arginine; NOS, nitric oxide synthase; H4biopterin, (6*R*,6*S*)-2-amino-4-hydroxy-6-(L-erythro-1,2-dihydroxypropyl)-5,6,7,8-tetrahydropteridine; [^{3}H]H4biopterin, biosynthetically labeled 6*R*-H4biopterin; SDS−PAGE, sodium dodecyl sulfate−polyacrylamide gel electrophoresis.

S0006-2960(97)00229-8 CCC: $14.00

attached as monomeric extensions that actually destabilize the dimeric structure (Ghosh & Stuehr, 1995; Ghosh et al., 1996). This model for iNOS structure is consistent with velocity sedimentation and dynamic light scattering data obtained with nNOS that indicates it may also have an elongated nonglobular shape (Klatt et al., 1995).

The individual NOS domains can be obtained by limited proteolysis of full-length enzymes or by expression in prokaryotic and eukaryotic cells (Ghosh & Stuehr, 1995; Sheta et al., 1994; Chen et al., 1996; McMillan & Masters, 1995; Salerno et al., 1996). In general, the domains have been found to maintain their native structures and properties. For example, the three NOS oxygenase domains maintain a dimeric structure, contain H4biopterin, bind L-arginine, and catalyze NO synthesis from either L-arginine or the reaction intermediate N^{ω}-hydroxyarginine (NOHA) when provided with their respective reductase domain and NADPH (Ghosh & Stuehr, 1995; Sheta et al., 1994; Chen et al., 1996; McMillan & Masters, 1995; Ghosh et al., 1995, 1996; Salerno et al., 1996). The iNOS oxygenase domain dimer (iNOSox) dissociates in the presence of urea into folded heme containing monomers (Ghosh et al., 1996). This transition is accompanied by loss of bound H4biopterin, a shift in heme iron spin state to low spin, and an increase in solvent access to the heme pocket, suggesting that dimeric structure and/or bound H4biopterin are important for maintaining the catalytic center of iNOS. Indeed, redimerization of iNOSox monomers reverses the changes in heme pocket structure and results in reincorporation of H4biopterin into the protein (Ghosh et al., 1996), while dimerization of urea-generated full-length iNOS monomers enables electron transfer between the flavins and heme iron and subsequent NO synthesis to occur (Abu-Soud et al., 1995; Siddhanta et al., 1996). NOS dimer assembly minimally requires that heme be incorporated into the subunits (Baek et al., 1993; Klatt et al., 1996). In the case of iNOS, dimerization of full-length or oxygenase domain monomers is promoted by H4biopterin and L-arginine (Baek et al., 1993; Ghosh et al., 1996), consistent with these molecules binding within the domain that participates in the dimeric interaction.

Although mutagenesis and homology studies have located the heme-binding cysteine in each NOS isoform (McMillan & Masters, 1995; Chen et al., 1994; Richards & Marletta, 1994; Sari et al., 1996; Renaud et al., 1993; Xie et al., 1996), the regions in the oxygenase domain that participate in dimeric interaction and/or H4biopterin and L-arginine binding have not been conclusively identified. Mutation of two highly conserved residues (G450A and A453I in the iNOS oxygenase domain) generated heme-containing mutants that were monomeric, did not incorporate H4biopterin or engage in NO synthesis (Cho et al., 1995). Because these two residues are located in a region that shares sequence homology with H4biopterin-utilizing amino acid hydroxylases, the authors speculated that G450 and A453 might participate in H4biopterin binding. Indeed, these residues lie within a larger conserved region in the C-terminal third of the oxygenase domain that bears some homology to the pterin binding module of dihydrofolate reductases (residues 339−491 in iNOS) (Nishimura et al., 1995). However, upon expressing the putative pterin binding module of nNOS as a fusion protein, these investigators found no evidence for H4biopterin interaction and instead found that it may bind *N*-nitroarginine (Nishimura et al., 1995). They concluded that the fragment either does not participate in binding H4biopterin or requires additional portions of the oxygenase domain to achieve this function. Consistent with these possibilities, point mutagenesis of eNOS at a cysteine residue (C99) that is conserved among the NOS's but located in a region of the oxygenase domain that bears no homology with pterin binding enzymes decreased eNOS affinity toward H4biopterin without affecting the enzyme's ability to bind L-arginine or catalyze NO synthesis (Chen et al., 1995). This suggests that a region in the NOS oxygenase domain located N-terminal from the heme coordination site may also be important for prosthetic group binding and domain function.

To address this issue, we have expressed a H4biopterin-free form of the iNOSox in *Escherichia coli* along with three point or N-terminal deletion mutants. On the basis of the spectroscopic, structural, catalytic, and ligand binding properties of these proteins as well as their susceptibility to limited proteolysis, we have identified a 49 amino acid segment located in the N-terminus of iNOSox that is involved in both subunit dimerization and productive H4biopterin interaction.

MATERIALS AND METHODS

Materials. DNA polymerase and other DNA modifying enzymes were obtained from Boehringer Mannheim or from Promega Biochemicals. Heme-free iNOS monomers were purified from the RAW 264.7 macrophage cell line as previously reported (Baek et al., 1993). A nickel-nitrilotriacetic acid (Ni-NTA) alkaline phosphatase conjugate used to identify the His_6-tagged proteins was from Qiagen. Site-specific oligonucleotide-directed mutagenesis was performed using the Altered Sites II in vitro mutagenesis system of Promega Biochemicals. Primers were synthesized by Life technologies. All other materials were obtained from Sigma Chemical or from sources previously reported (Ghosh & Stuehr, 1995; Ghosh et al., 1996). Amino acid sequencing was performed at Berlex Biosciences, Richmond, CA.

Cloning of the iNOSox. The cDNA encoding amino acids 1−498 of mouse iNOS was modified by PCR to contain an *Nde*I site and a His_6 leader sequence at the 5′ end and a *Sal*I site at the 3′ end. The iNOSox cDNA was then cloned into a similarly restricted pCWori expression vector (McMillan & Masters, 1995; Wu et al., 1996). DNA sequence was checked at the core facility of the Cleveland Clinic.

Deletion and Site-Directed Mutagenesis of iNOSox. The iNOSox cDNA was cloned into the pALTER-1 mutagenesis vector at its *Sma*I 1 site. Single-stranded DNA was prepared as the template for site-directed mutation. The C109A mutant was constructed by oligonucleotide-directed mutagenesis according to the protocol included in the Altered Sites II in vitro mutagenesis system. The oligonucleotide 5′-AAGTCCAAGTCTGCCTTGGGGTCC-3′ contains a TG to GC substitution in the first and second bases of the codon of amino acid 109 to produce the C109A mutation. Deletion mutants Δ65 and Δ114 were constructed by PCR using 5′-end deletion primers AATGTTCCAGAA<u>CATATG</u>GACAAGCTG for removing residues 1−65 and TGCTTGGGGTCC<u>CATATG</u>AACCCC for removing residues 1−114. In both cases, the 3′-end primer AGTTGTGCATCGACCTAGGCTGG was used to incorporate an *Avr*2 unique restriction site in the iNOSox sequence at residue 243. PCR products and pCWori plasmid DNA were cut with *Nde*1 at the 5′-end and *Avr*2 at the 3′-end, then ligated at 14 °C overnight. The DNA sequence of all mutants was confirmed by nucleotide sequencing, and deletion mutants were also checked following expression by N-terminal protein sequencing.

Protein Expression and Purification. Plasmids (pCWori) containing iNOSox or mutants C109A, Δ65 and Δ114 cDNAs were transformed into protease-deficient *E. coli* BL21(DE3). The cultures were grown with shaking at 250 rpm at 25 °C. Expression of protein was induced by adding 1 mM isopropylthio-*β*-D-galactoside (IPTG) to the culture when it reached an optical density of 1 at 600 nm, and Δ-aminolevulinic acid was also added at this point to give a final concentration of 450 *μ*M. Cells were harvested 48 h after induction by centrifugation at 3600 rpm for 15 min. The cells from 4 L of culture were suspended in minimum volume of lysis buffer containing 40 mM *N*-(2-hydroxyethyl)piperazine-*N′*-(3-propane sulfonic acid) (EPPS), pH 7.6, 0.5 mg/mL lysozyme, 10% glycerol, 0.5 *μ*g/mL each of leupeptin, pepstatin, and phenylmethanesulfonyl fluoride (PMSF), 1.0 mM L-arginine, and 0.25 M NaCl. Cells were broken by sonication (three 10 s pulses) followed by three cycles of freezing and thawing in liquid N_2 and at 37 °C, respectively. The suspension was centrifuged at 13 200 rpm for 25 min to remove cell debris, and the cytochrome P-450 concentration of the supernatant was checked. The crude extract was loaded onto a Ni-NTA Sepharose 4B column (2.5/10 cm) previously charged with 50 mM NiSO4 and equilibrated with 40 mM EPPS buffer, pH 7.6, containing 10% glycerol, 1 mM PMSF, and 0.25 M NaCl (buffer A). The column was then washed with 10 bed volumes of buffer A and 5 vol of buffer A containing 40 mM imidazole. Bound protein was eluted with buffer A containing 150−200 mM imidazole. Column fractions containing iNOSox were pooled and concentrated using a centriprep-30 (Millipore). The concentrated proteins were dialyzed at 4 °C against two 500 mL vol of 40 mM EPPS, pH 7.6, containing 10% glycerol, and 1 mM DTT in presence or absence of 4 *μ*M H4biopterin, and stored in aliquots at −70 °C.

UV−Visible Spectroscopy. Measurements were obtained on a Hitachi U3110 spectrometer equipped with computer assisted data collection software (Galactic Industries). Spectra were obtained on proteins dissolved in 40 mM EPPS, pH 7.6, containing 5% glycerol and 1 mM DTT or 2 mM *β*-mercaptethanol (BME). The Soret absorbance band of the iNOSox ferrous−carbon monoxide adduct was used to quantitate the hemeprotein, using an extinction coefficient of 74 mM^{-1} cm^{-1} (444−500 nm) (Stuehr & Ikeda-Saito, 1992). In certain experiments, the time course of spectral change associated with H4biopterin or L-arginine binding at 30 °C was monitored at 400 nm under conditions noted in the text.

L-Arginine binding affinity was studied by perturbation difference spectroscopy according to methods described previously (McMillan & Masters, 1993; Ghosh et al., 1996). Binding was studied at 30 °C using protein preparations that had been dialyzed in 40 mM EPPS, pH 7.6, containing 5% glycerol and 2 mM BME. Concentrations of H4biopterin and imidazole were added to the cuvette prior to titration with L-arginine (0−1 mM) as noted in the text. Spectra were recorded after each addition of L-arginine. The final sample volume change was less than 5%.

Binding of ^{3}H-Labeled H4biopterin. Binding of H4biopterin to iNOSox and mutants was investigated as described previously for purified nNOS (Klatt et al., 1994) with modifications. For saturation binding, purified iNOSox (18 pmol) was incubated 45 min at 37 °C with 20 nM (∼18 nCi) of [^{3}H]H4biopterin and increasing concentrations (0−1 mM) of unlabeled H4biopterin or pterin analogs in 1 mL of 50 mM triethanolamine-HCl buffer, pH 7.4, containing 0.1 mM DTT. In some cases, 0.1 mM L-arginine or NOHA was also present in the incubations. Separation of bound from free ligand was performed by polyethylene glycol precipitation followed by vacuum deposition of the protein on Whatman glass fiber filter paper and washing the precipitate twice under vacuum with 100 *μ*L of buffer. Bound radioactivity was determined by scintillation counting. Data were corrected by subtracting nonspecific binding which was determined in incubations containing 20 nM [^{3}H]H4biopterin and 1 mM (50000-fold excess) of unlabeled H4biopterin. The amount of total H4biopterin specifically bound to iNOSox (labeled plus unlabeled) was determined by the following calculation which takes into account nonspecific binding and the dilution of label at each H4biopterin concentration used in the experiment:

$$\text{H4biopterin}_{sb} = (\text{dpm measured} - \text{dpm nonspecific})\ (\text{total H4biopterin concentration}/20\ \text{nM})(0.50\ \text{fmol}\ [3\text{H}]\text{H4biopterin}/\text{dpm})$$

The amount specifically bound was then normalized for the amount of protein and usually reported as picomoles bound per nanomole iNOS protein. K_d and B_{max} values were determined using the GIPMAX nonlinear least-squares regression curve fitting program (Brunner & Kukovetz, 1991). Association kinetics were determined at 4 °C by adding 20 nM [^{3}H]H4biopterin to 1 mL incubation buffer containing 10−20 *μ*g of iNOSox (or mutants) and immediately removing and processing 0.1 mL aliquots for bound counts at the indicated times. Dissociation kinetics were determined at 4 °C in 1 mL incubation buffer as above except in this case iNOSox or mutants were preincubated 45 min with 20 nM [^{3}H]H4biopterin followed by addition of 1 mM unlabeled H4biopterin to start the dissociation reaction. Aliquots (0.1 mL) were removed at the indicated times and processed immediately as described above.

Limited Proteolysis. Limited trypsin digestion of iNOSox dimer, monomer, selected mutants, or heme-free full-length iNOS monomer was carried out on ice in 40 mM EPPS, pH 7.6, containing 1 mM DTT and 5% glycerol, at a protein to trypsin ratio of 25:1 (w/w). At regular intervals for up to 2 h, 10 *μ*g of the protein was removed from each incubation, immediately boiled with Laemmli sample buffer, and saved on ice for analysis on 10% SDS−PAGE, according to methods described earlier (Ghosh & Stuehr, 1995). In some cases, protein samples were preincubated with various concentrations of H4biopterin and/or L-arginine before adding trypsin.

Gel Filtration Analysis. Native molecular weight of proteins or protein fragments was estimated by size exclusion chromatography, using a Pharmacia Superdex 200 HR column equilibrated with 40 mM EPPS, pH 7.6, containing 10% glycerol, 0.5 mM DTT, and 0.2 M NaCl. Protein in the column effluent was detected at 280 nm using a flow-through detector. The molecular weight of the protein peaks was estimated relative to gel filtration molecular weight standards as previously described (Abu-Soud et al., 1995; Ghosh et al., 1996).

Catalysis of NOHA Oxidation by iNOSox. The H_2O_2-supported oxidation of NOHA by iNOSox or related proteins was measured as nitrite formed in a 10 min reaction at 37 °C, according to the procedure described by Pufahl et al. (1995), with slight modification. The reaction was carried out in 100 μL of total volume containing 40 mM Hepes, pH 7.5, 150 nM iNOSox, 1 mM NOHA, 0.5 mM DTT, 30 mM H_2O_2, 10 units/mL superoxide dismutase, 0.5 mg/mL bovine serum albumin, and variable concentrations of H4biopterin (0−300 μM). The reaction was initiated by adding H_2O_2 and stopped after 10 min by adding catalase (13 units/μL). An equal volume of Griess reagent (100 μL) was then added to detect nitrite colorimetrically at 550 nm, and quantitated based on sodium nitrite standards.

Preparation of Urea Monomers and Their Association. Monomers of iNOSox and of related dimeric proteins were prepared by incubating them for 2 h at 4 °C in 40 mM EPPS buffer, pH 7.6, containing 5 M urea and 2 mM DTT (Abu-Soud et al., 1995; Ghosh et al., 1996). The urea concentration was then reduced either by diluting the samples 10-fold in buffer without urea (Siddhanta et al., 1996) or by sequential dialysis for 2 h against 500 mL buffer containing 2 M urea followed by overnight dialysis in 500 mL buffer containing 0.1 M urea (Ghosh et al., 1996). Either method generated preparations that were 80−90% monomeric as judged by gel filtration analysis. Dimerization of monomers was done by incubating the monomers (1.5−2.5 μM) for 30−90 min at 37 °C in 40 mM EPPS buffer, pH 7.6, containing 3 mM DTT, 10−200 μM H4biopterin, and 5 mM L-arginine. In some cases, incubations were run in cuvettes or microwells to monitor the changes in visible absorbance at 400 nm versus time during the dimerization incubation. In some cases, additives were omitted from the incubations as described in the text. Samples were analyzed by gel filtration chromatography at the end of each incubation according to methods described earlier (Ghosh et al., 1996).

RESULTS

Characterization of iNOSox Expressed in E. coli. The mouse iNOSox (residues 1−498) was overexpressed in *E. coli* as a C-terminal His_6-tagged protein using the expression vector pCWori, which has previously been used to express all three full-length NOSs (Wu et al.,1996; Roman et al., 1995; Gerber & Ortiz de Montellano, 1995; Rodriguez-Crespo et al., 1996; Martasek et al., 1996; Fossetta et al., 1996) and the nNOS oxygenase domain (McMillan & Masters, 1995). The expression system generated 15−20 mg of iNOSox protein/L of culture, of which 60−80% could be purified by Ni-NTA Sepharose chromatography. The iNOSox had an apparent molecular weight of 55 000, as determined by SDS−PAGE, was immunoreactive toward anti-mouse iNOS IgG, and contained approximately 1 heme/molecule of protein as determined by the hemechromogen assay (Stuehr & Ikeda-Saito, 1992) (data not shown). Sequence analysis indicated that N-terminal microheterogeneity was present in iNOSox due to proteolysis, and attempts to reduce or prevent this proteolysis by inclusion of protease inhibitors or expression in protease-deficient strains of *E. coli* were unsuccessful. The major species present in our iNOSox preparations were the N-terminal deletions Δ13 (56%) and Δ34 (28%), while the minor species were Δ54 (8%), Δ7 (8%), and Δ6 (4%). However, these deletions all occur within a region of low sequence homology between the NOS isoforms, which extends from residues 1 to 75 in mouse iNOS (Reguliski & Tully, 1995).

Gel filtration analysis of iNOSox samples that were prepared either in the presence or absence of H4biopterin showed that at least 80% of the total protein was dimeric in both cases (data not shown). Overexpression of iNOSox in *E. coli* therefore contrasts with mammalian expression of full-length iNOS, where assembly of the dimer is greatly facilitated by concurrent H4biopterin biosynthesis (Tzeng et al., 1995). The dithionite-reduced iNOSox exhibited a Soret peak at 414 nm which shifted to 444 nm upon binding CO, indicating that its heme iron is ligated to a cysteine thiolate, as in native iNOSox (Stuehr & Ikeda-Saito, 1992; Ghosh et al., 1995). The ferrous−carbon monoxide complex was stable under anaerobic conditions in the presence of L-arginine and H4biopterin, but was unstable in the absence of these molecules and converted to a P-420-like species over time (data not shown). In the presence of H4biopterin and H_2O_2, iNOSox catalyzed NO and citrulline synthesis from NOHA at an initial rate of 18.2 μM nitrite/min/μg oxygenase domain, which is comparable to the rate reported for full-length iNOS under similar conditions (Pufahl et al., 1995).

H4biopterin and L-arginine binding to iNOSox was investigated by spectral perturbation analysis (Ghosh et al., 1996; McMillan & Masters, 1993), using protein preparations that were either dialyzed against 2 mM BME (Figure 1, panel A) or dialyzed against 1 mM DTT (Figure 1, panels B−D). In the BME-dialyzed preparation, the spectral changes obtained upon addition of H4biopterin indicate that its binding caused a partial shift from a low-spin, six-coordinate heme to a high-spin, five-coordinate heme (Figure 1, panel A and inset). Subsequent addition of L-arginine caused a further shift to the high-spin species. The DTT-dialyzed iNOSox preparation exhibited a split Soret absorbance at 460 and 380 nm, indicating a thiolate from DTT was coordinating directly to the heme iron of iNOSox to form a six-coordinate bisthiolate species (Abu-Soud et al., 1995; Sono et al., 1982). H4biopterin partially displaced the DTT ligand and caused a partial conversion to the five-coordinate, high-spin species, with subsequent addition of L-arginine causing full displacement of DTT and conversion to high-spin (Figure 1, panel B and inset). Adding L-arginine alone also displaced the DTT ligand and caused a similar change in heme iron spin state (Figure 1, panel C). However, the rate of spectral change in this case was much slower than in samples that had received H4biopterin, and required overnight incubation to reach equilibrium (Figure 1, panel D).

We quantitated binding of H4biopterin and two related dihydropterins to iNOSox utilizing equilibrium methods and [^{3}H]H4biopterin as a radioligand (Klatt et al., 1994). As listed in Table 1, iNOSox exhibited a submicromolar affinity constant toward H4biopterin, which decreased in magnitude almost 5-fold in the presence of 0.1 mM L-arginine or the reaction intermediate NOHA. A similar synergy in binding H4biopterin and L-arginine has also been observed with neuronal NOS (Klatt et al., 1994) and full-length iNOS.[2] Unlabeled dihydropterins (dihydrobiopterin and sepiapterin) competed with [^{3}H]H4biopterin for binding to iNOSox and gave estimated K_d's in the micromolar range, with affinities increasing 2- to 3-fold in the presence of L-arginine or NOHA. Kinetic analysis of [^{3}H]H4biopterin association/dissociation to iNOSox is shown in Figure 2, and gave k_{on} = $(3.4 \pm 0.4) \times 10^5$ M^{-1} min^{-1} and k_{off} = $(7.8 \pm 2.1) \times$

[2] Mayer, B., Wu, C., Gorren, A. C. F., Ghosh, D. K., Pfeiffer, S., Schmidt, K., Werner, E. R., & Stuehr, D. J. *Biochemistry* (in press).

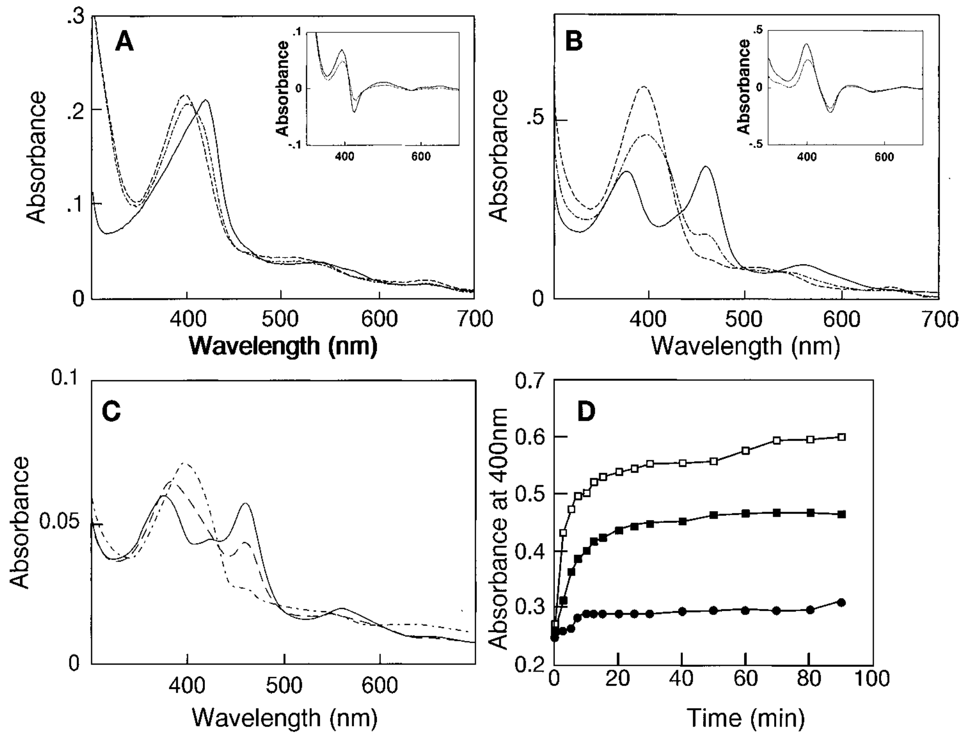

FIGURE 1: Light absorbance spectra of iNOSox prior to and following binding of H4biopterin and L-arginine at 30 °C. Panel A depicts spectra of 3 μM iNOSox recorded sequentially after dialysis in 40 mM EPPS buffer, pH 7.6, containing 5% glycerol (v/v) and 2 mM BME (—); after a subsequent 20 min incubation with 10 μM H4biopterin (-•-•-); and after a subsequent 20 min incubation with H4biopterin and 5 mM L-arginine (- - -). The inset shows the difference spectra generated by subtracting the initial spectrum from that recorded after the H4biopterin incubation (•••) or after incubation with H4biopterin plus L-arginine (—). Panel B depicts spectra of 8 μM iNOSox after dialysis under conditions identical to panel A except that 1 mM DTT replaced BME (—). Information pertaining to each sequential scan, the inset difference spectra, and line designations are as described for panel A. Panel C depicts spectra of 1.0 μM iNOSox recorded sequentially after dialysis in 40 mM EPPS buffer, pH 7.6, containing 5% glycerol (v/v) and 1 mM DTT (—); after a subsequent 90 min incubation with 10 mM L-arginine at 30 °C (- - -), and after additional incubation with 10 mM L-arginine for 16 h at 4 °C (-•-•-). Panel D shows the kinetics of spectral change at 30 °C upon addition of 10 mM L-arginine (●), 10 μM H4biopterin (■), or L-arginine plus H4biopterin (□) to three separate samples of 8 μM iNOSox in 40 mM EPPS buffer, pH 7.6, containing 5% glycerol and 1 mM DTT. Spectra were recorded at the times indicated by each symbol to obtain the absorbance values at 400 nm.

Table 1: Pterin Binding by iNOSox[a]

	no substrate		0.1 mM L-arginine		0.1 mM NOHA	
unlabeled ligand	K_d (K_i), μM	B_{max}[b]	K_d (K_i), μM	B_{max}	K_d (K_i), μM	B_{max}
H4biopterin	0.25 ± 0.04	61 ± 8	0.06 ± 0.01	83 ± 2	0.06 ± 0.01	139 ± 9
H2biopterin	1.0 ± 0.1	98 ± 3	0.7 ± 0.1	72 ± 10	0.4 ± 0.1	93 ± 5
sepiapterin	47 ± 6	109 ± 7	12 ± 3	64 ± 13	17 ± 4	77 ± 5

[a] Values were obtained from experiments in which 18 pmol of iNOSox (18 nM) was incubated for 45 min at 37 °C with 20 nM [^{3}H]H4biopterin and varying concentrations of unlabeled ligand as described in Materials and Methods. In some cases, the incubations also contained L-arginine or NOHA. After incubation, specifically bound H4biopterin was determined as described in Materials and Methods and binding constants were derived by plotting bound H4biopterin (labeled plus unlabeled) versus ligand concentration (Klatt et al., 1996). Values represent the mean ± SD for three determinations. [b] B_{max} is picomoles of H4biopterin bound per nmol iNOSox monomer.

10^{-3} min^{-1}, respectively. In general, pterin binding by iNOSox was similar to that reported for full-length nNOS (Klatt et al., 1994), except that the dissociation rate of H4biopterin from iNOSox is slow when compared to nNOS.

Proteolytic Susceptibility and Characterization of Δ117 iNOSox. We next utilized ligand protection against proteolysis as a probe to identify what regions may be involved in H4biopterin or L-arginine interaction with iNOSox. Structural analysis based on susceptibility to proteolysis has proven generally useful because proteolysis depends on the accessibility of scissile bonds, which in turn is directly dependent on structure. This method has frequently been used to study protein conformational changes associated with function (Liu et al., 1995; Gibbs et al., 1988; Inaba & Mohri, 1989; Betton et al., 1989; Caroll et al., 1994; Tsokos et al., 1992) and to compliment absorbance or fluorescence investigations.

We reported previously that limited trypsin proteolysis of H4biopterin-replete full-length iNOS cleaved the protein into its two domains at residue R503, generating an iNOSox dimer that was resistant to further proteolysis by trypsin (Ghosh & Stuehr, 1995). However, as shown in Figure 3, the H4biopterin- and L-arginine-free iNOSox dimer (denatured molecular mass of 55 kDa, lane 2) contained one additional trypsin-sensitive site whose cleavage generated a protein fragment of ~40 kDa (lane 3). Identical results were obtained when starting with heme-containing iNOSox monomers (data not shown),[3] suggesting that dimeric structure alone does not influence the trypsin susceptibility of this site.

[3] Under identical conditions, heme-free iNOS monomers are cut by trypsin throughout the oxygenase domain at residues 107, 117, 197, and 382 (D. K. Ghosh, T. Slattery, and D. J. Stuehr, unpublished observation).

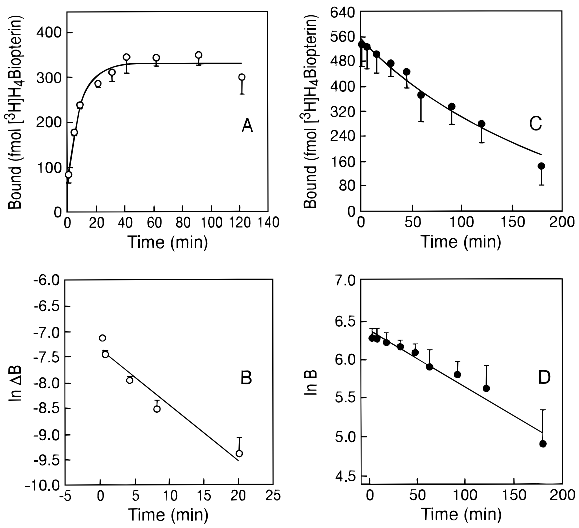

FIGURE 2: Association and dissociation kinetics of [^{3}H]H4biopterin binding to iNOSox. Panel A shows the kinetics of [^{3}H]H4biopterin binding to iNOSox at 4 °C. Incubations contained 10 μg (180 pmol) of iNOSox and 20 nM [^{3}H]H4biopterin in 1 mL. At indicated time points, 0.1 mL aliquots were removed assayed for bound radioactivity using protein precipitation and deposition on glass fiber filters as described in Materials and Methods. Nonspecific binding was determined in the presence of 1 mM unlabeled H4biopterin and was between 2−3% of the total radioactivity and subtracted from each total bound value. Panel B represents the plot of binding data according to the second-order rate law. The term ln ΔB represents $\ln[(X_{eq}-X_t)/(\text{iNOSox} \times \text{H4biopterin} - X_{eq} \times X_t)]$ where X refers to the molar concentration of specifically bound [^{3}H]H4biopterin at equilibrium ($t \geq 45$ min) and time t (t), respectively. iNOSox and H4biopterin are the initial molar concentrations of iNOS and [^{3}H]H4biopterin at $t = 0$, respectively. Panel C depicts the dissociation kinetics of [^{3}H]H4biopterin binding from iNOSox. After a 45 min of incubation with 20 nM [^{3}H]H4biopterin at 4 °C, the dissociation was initiated by addition of 1 mM unlabeled H4biopterin. At the time points indicated aliquots (0.1 mL) were removed and [^{3}H]H4biopterin that had remained bound to iNOSox was determined by scintillation counting. Panel D replots the dissociation data according to a first-order rate law. B refers to the amount of bound [^{3}H]H4biopterin expressed in femtomoles per assay. The plots shown are representative of three.

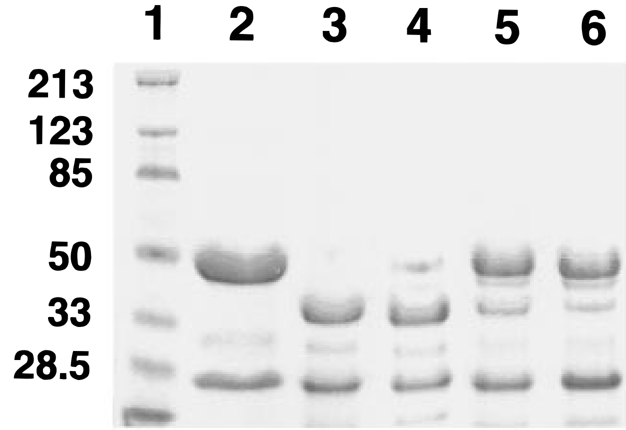

FIGURE 3: Ability of L-arginine or H4biopterin to protect the iNOSox dimer from limited trypsin digestion. The iNOSox was dialyzed against 40 mM EPPS, pH 7.6, containing 5% glycerol and 1 mM DTT, and then preincubated for 16 h at 4 °C either in this buffer alone or in buffer containing 10 mM L-arginine, 10 μM H4biopterin, or 10 mM L-arginine plus 10 μM H4biopterin. The light absorbance spectrum of each protein sample was recorded after preincubation to ensure spectral changes associated with binding had occurred (see Figure 1). Proteolysis was then carried out on ice for 2 h, and the samples were boiled with Laemmli buffer and analyzed by SDS−PAGE. Lanes 1, molecular weight standards, 2, iNOSox standard, and 3−6, trypsin-digested iNOSox preincubated in buffer alone, L-arginine alone, H4biopterin alone, or a combination of L-arginine plus H4biopterin, respectively. The protein band of estimated molecular mass 25 kDa was identified by microsequencing to be a contaminant protein (chloramphenicol-acyl transferase derived from *E. coli*). The experiment shown is representative of five similar experiments.

Attempts to isolate the complimentary 15 kDa fragment by gel filtration chromatography indicated that it was not present in intact form and therefore likely underwent additional proteolysis. The 40 kDa protein was reactive toward Ni-NTA alkaline phosphatase conjugate (data not shown), confirming that its C-terminus was still intact. N-terminal sequence analysis of the 40 kDa protein revealed that >99% of the iNOSox had been cleaved at residue K117, thus generating the deletion Δ117 iNOSox.

To determine if bound L-arginine or H4biopterin could protect iNOSox against trypsin proteolysis at this site, we incubated iNOSox samples overnight with 10 mM L-arginine or 10 μM H4biopterin before exposing them to trypsin. The L-arginine-saturated iNOSox was not protected from trypsin cleavage (Figure 3, lane 4), whereas iNOSox samples saturated with H4biopterin alone (lane 5) or with H4biopterin plus L-arginine (lane 6) were significantly protected from cleavage. We conclude that bound H4biopterin, but not bound L-arginine, shields the iNOSox dimer from proteolytic cleavage at K117, which is located N-terminal from the heme-binding residue C194 (Xie et al., 1996).

Analysis of Δ117 iNOSox following its purification by gel filtration chromatography revealed it had maintained bound heme and was present as a bis-thiolate complex with DTT (Figure 4, panel A). Although bound DTT could be displaced by imidazole, it could not be displaced by L-arginine plus H4biopterin. Delta 117 iNOSox was also unable to bind [^{3}H]H4biopterin or catalyze NO synthesis from NOHA in the H_2O_2-supported reaction (data not shown). Dithionite reduction of Δ117 iNOSox followed by CO binding initially generated the thiolate-ligated six-coordinate ferrous−carbon monoxide species that absorbs at 444 nm, but the complex was unstable and converted to a P-420 species with time (Figure 4, panel B). Gel filtration analysis showed the Δ117 iNOSox was completely monomeric (Figure 4, panel A inset), and in contrast to normal heme-containing iNOSox monomers (Ghosh et al., 1996) did not dimerize when incubated with H4biopterin and L-arginine (data not shown). Thus, proteolytic removal of the first 117 residues in an iNOSox dimer converted it into a heme-containing monomer that could not productively interact with L-arginine and H4biopterin as judged by several criteria.

Characterization of Δ65, Δ114, and C109A iNOSox. We constructed N-terminal deletion mutants of iNOSox that were missing the first 65 residues (Δ65 iNOSox) or 114 residues (Δ114 iNOSox) and a point mutant (C109A) to investigate further a role for the N-terminal region in dimeric interaction and L-arginine or H4biopterin binding. The Δ65 deletion removes residues that lie within a region of low homology between the NOS isoforms (represented by residues 1−75 in iNOS), while the Δ114 deletion removes residues up to a point that is close to the trypsin cleavage site in iNOSox at residue K117. The C109A point mutation eliminates a conserved cysteine that is located close to the site of proteolytic cleavage in iNOSox and has been reported to modulate H4biopterin binding affinity in bovine endothelial NOS (Chen et al., 1995).

Spectroscopic characterization of Δ65 iNOSox showed that it bound H4biopterin and L-arginine (Figure 5, panel

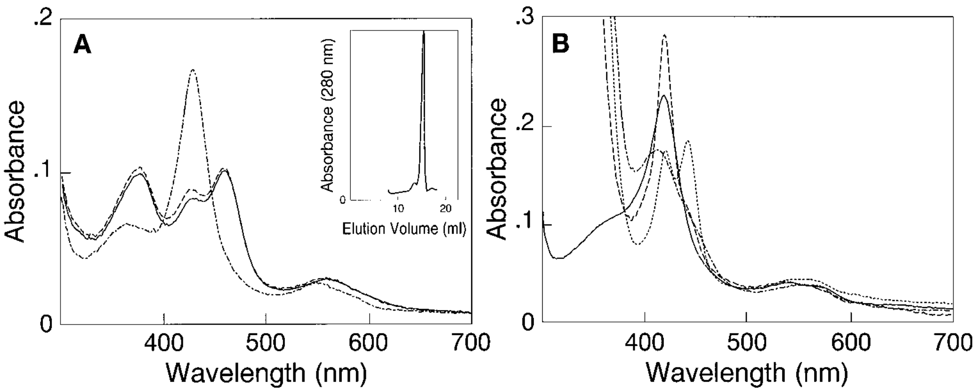

FIGURE 4: Characterization of trypsin-generated Δ117 iNOSox. Panel A shows the light absorbance spectra of three separate samples of 1.5 μM Δ117 iNOSox in 40 mM EPPS buffer, pH 7.6, containing 5% glycerol and 1 mM DTT. Buffer alone (—); in the presence of 10 mM L-arginine and 300 μM H4biopterin (- - -); and in the presence of 400 μM imidazole (-•-•-). The inset shows the gel filtration profile of Δ117 iNOSox, eluting as a monomer at 15 mL. Panel B shows light absorbance spectra for a single sample of 1.5 μM Δ117 iNOSox in 40 mM EPPS buffer containing 5% glycerol and 2 mM BME. Spectra were recorded sequentially and under anaerobic conditions at 15 °C. Ferric Δ117 iNOSox (—); after reduction to ferrous with dithionite (-•-•-); immediately after adding CO (- - -); and 20 min later (- -).

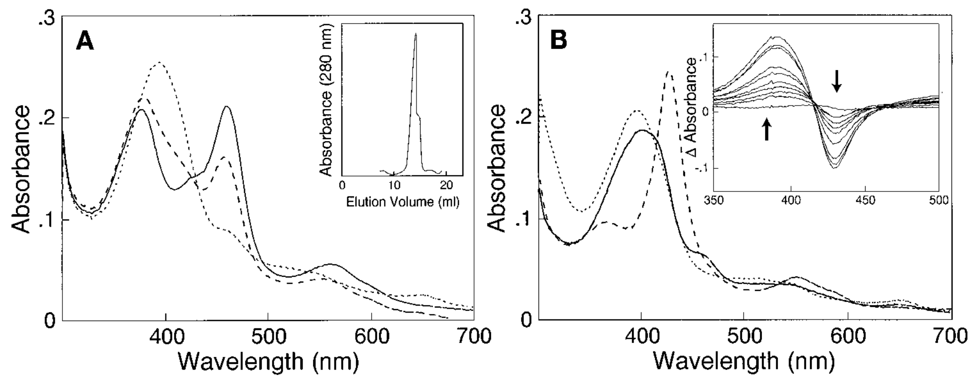

FIGURE 5: Characterization of Δ65 iNOSox. Panel A shows light absorbance spectra of 2 μM Δ65 iNOSox in 40 mM EPPS buffer, pH 7.6, containing 5% glycerol and 1 mM DTT (—); after incubating this sample with 10 mM L-arginine for 90 min at 30 °C (- - -); and after incubating it an additional 16 h with L-arginine at 4 °C (•••). The inset shows the gel filtration profile of Δ65 iNOSox, eluting predominantly as a dimer at 13 mL. Panel B shows light absorbance spectra recorded sequentially for a single sample of 1.5 μM Δ65 iNOSox at 30 °C. The protein equilibrated in 40 mM EPPS buffer containing 5% glycerol, 2 mM BME, and 10 μM H4biopterin (—); after subsequent addition of 400 mM imidazole (- - -); and after subsequent titration of this sample with L-arginine, only the spectrum obtained at 1 mM L-arginine is shown (•••). The inset contains the perturbation difference spectra generated after each addition of L-arginine starting from 3 μM to 1 mM. The data shown are representative of duplicate experiments. The spectral binding constant for L-arginine was determined from a double reciprocal plot of the absorbance change at 390−430 nm versus L-arginine concentration.

A), was primarily dimeric (Figure 5, panel A inset), was resistant to proteolysis in the presence of H4biopterin (data not shown), and could catalyze NO synthesis from NOHA in the H_2O_2-supported reaction as well as wild-type iNOSox (see Figure 7). We quantitated its L-arginine binding affinity by spectral perturbation in the presence of 400 μM imidazole (Figure 5, panel B) and its affinity toward H4biopterin using the radioligand binding assay. Delta 65 iNOSox had a spectral binding constant for L-arginine of 11 μM, which is similar to wild-type iNOSox when assayed under identical conditions (Ghosh & Stuehr, 1995; Ghosh et al., 1996) and displayed an affinity toward H4biopterin similar to wild-type [$K_d = 0.1\ \mu$M; $k_{on} = (3.4 \pm 0.3) \times 10^5$ M^{-1} min^{-1}, $k_{off} = (3.4 \pm 0.3) \times 10^{-3}$ min^{-1}]. In contrast, Δ114 iNOSox did not interact with added L-arginine and H4biopterin as judged either by spectral perturbation or by [H^3]H4biopterin binding (data not shown). As shown in Figure 6, Δ114 iNOSox was isolated as a monomer−dimer mixture (trace 1) which did not dimerize further in the presence of added H4biopterin and L-arginine (trace 2) and could be cleaved by trypsin even in the presence of H4biopterin to generate the completely monomeric Δ117 iNOSox as a product (trace 3). Thus, Δ65 iNOSox appeared to be identical to wild-type, while Δ114 iNOSox was similar to the trypsin-generated Δ117 iNOSox, with the exception of its maintaining some dimeric structure.

The C109A iNOSox point mutant was ∼80% dimeric following its purification in the absence of H4biopterin and L-arginine (data not shown). We analyzed its H4biopterin binding by spectral perturbation and by radioligand binding. Added H4biopterin gradually displace DTT as a heme iron ligand to generate five-coordinate high-spin heme, indicating that it bound to C109A iNOSox (data not shown). The binding constants derived from radioligand binding data gave a H4biopterin K_d of 0.82 ± 0.08 μM in absence of L-arginine with $k_{on} = 1.7 \times 10^4$ M^{-1} min^{-1}, $k_{off} = 1.4 \times 10^{-2}$ min^{-1}, and a K_d of 0.40 ± 0.03 μM in the presence of 0.1 mM L-arginine with $k_{on} = 1.5 \times 10^5$ M^{-1} min^{-1}, and $k_{off} = 6.0 \times 10^{-3}$ min^{-1}. We conclude that C109A iNOSox exhibits a decreased affinity toward H4biopterin due to both a decreased rate of H4biopterin association and increased rate of dissociation relative to wild-type iNOSox.

To further probe H4biopterin's interaction with C109A iNOSox, we examined the ability of H4biopterin to support NO synthesis from NOHA, provide protection against trypsin proteolysis, and promote dimerization of urea-generated monomers. Figure 7 shows NO synthesis from NOHA at different H4biopterin concentrations for C109A, wild-type,

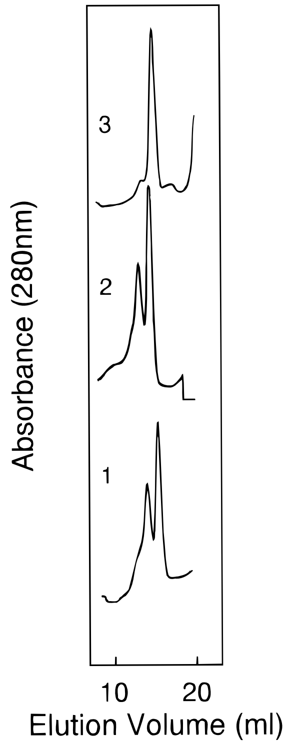

FIGURE 6: Gel filtration analysis of Δ114 iNOSox. Trace 1, the protein as isolated is a mixture of dimer and monomer eluting at 13 and 15 mL, respectively. Trace 2, the elution profile following a 2 h incubation with 100 μM H4biopterin and 10 mM L-arginine. Trace 3, the elution profile after trypsin digestion for 30 min at 4 °C in the presence of 100 μM H4biopterin and 10 mM L-arginine. The data is representative of three similar experiments.

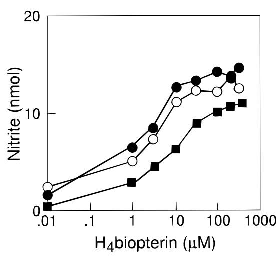

FIGURE 7: Catalysis of NOHA oxidation as a function of H4biopterin concentration for iNOSox (●), Δ65 iNOSox (○), and C109A iNOSox (■). Nitrite values are the amount formed in a 10 min reaction at 30 °C. Proteins were preincubated for 30 min with the indicated concentrations of H4biopterin before initiating the reaction with H_2O_2. The points are the mean ± SD of reactions done in triplicate.

and Δ65 iNOSox. Double reciprocal analysis gave apparent K_m and V_{max} values for C109A of 10.5 ± 0.6 μM and 0.9 nmol/min, respectively. These differed from apparent K_m values calculated for wild-type and Δ65 iNOSox (K_ms = 1.2 ± 0.2 and 1.4 ± 0.3 μM; V_{max} = 1.4 and 1.3 nmol/min, respectively). A higher concentration of H4biopterin (>100 μM) was also required to fully protect the C109A iNOSox dimer from trypsin proteolysis as compared to wild-type iNOSox (10 μM H4biopterin) (data not shown).

Dimerization of urea-generated iNOSox monomers can be followed in the presence of DTT as an absorbance increase at 400 nm that is due to displacement of DTT from the dimeric iNOSox heme iron (Ghosh et al., 1996). On the basis of the absorbance changes shown in Figure 8, panel A, dimerization of wild-type iNOSox monomers under ideal conditions (10 μM H4biopterin plus 5 mM L-arginine) neared

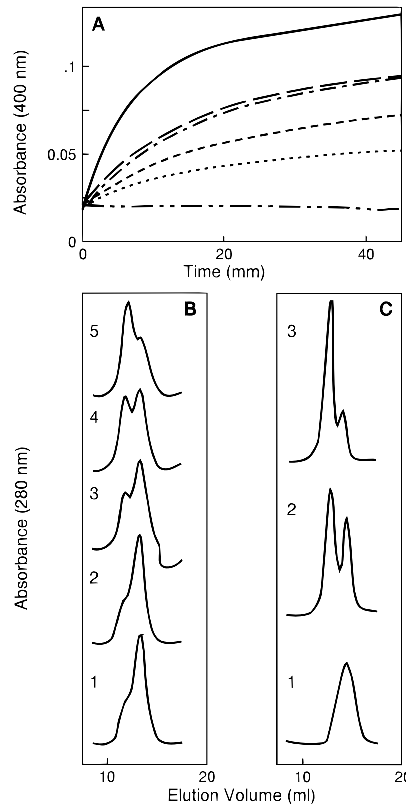

FIGURE 8: Kinetics and extent of dimerization for monomers of wild-type and C109A iNOSox under various incubation conditions. Panel A follows dimerization as the change in absorbance at 400 nm versus time for incubations containing 1.7 μM iNOSox plus 10 μM H4biopterin and 5 mM L-arginine (—), 10 μM H4biopterin alone (- -); or an equivalent concentration of C109A iNOSox plus 100 μM H4biopterin and 5 mM L-arginine (-•-•-), 200 μM H4biopterin alone (- - -), 100 μM H4biopterin alone (•••), and 10 μM H4biopterin alone (-••-). Panels B and C depict the corresponding gel filtration profiles of C109A (panel B) or wild-type (panel C) iNOSox monomers that had been incubated for 45 min with no additives (1), 10 μM H4biopterin (2), 100 μM H4biopterin (B3), 200 μM H4biopterin (4), 100 μM H4biopterin plus 5 mM L-arginine (5), and 10 μM H4biopterin plus 5 mM L-arginine (C3). The data is representative of two or three experiments.

completion within 20 min and resulted in an absorbance increase at 400 nm of approximately 0.1 unit. When 10 μM H4biopterin was provided in the absence of L-arginine, spectral change associated with iNOSox dimer assembly still occurred but to a lesser extent. With urea-generated C109A monomers, an absorbance change indicative of dimerization was not observed at 10 μM H4biopterin, but was observed in a concentration-dependent manner at 100 and 200 μM H4biopterin (Figure 8, panel A). Providing both 5 mM L-arginine and 100 μM H4biopterin to the C109A monomers resulted in an absorbance increase that was still below that obtained for wild-type iNOSox under similar conditions, suggesting incomplete dimerization of C109A monomers occurred even under these conditions. Gel filtration profiles of the six dimerization incubations of Figure 8, panel A, are illustrated in panel B for the C109A iNOSox incubations and panel C for the wild-type iNOSox incubations. The proportions of dimer and monomer present at the end of each incubation as determined by gel filtration are consistent with the absorbance changes in panel A and confirm that C109A monomers require elevated concentrations of H4biopterin to achieve a given degree of dimerization.

DISCUSSION

Expression of iNOSox in *E. coli* enabled us to characterize the protein in its H4biopterin-free form, which is not normally available from eukaryotic expression systems (Tzeng et al., 1995; Gross & Levi, 1992). The H4biopterin-free iNOSox was similar to conventional iNOSox in being mostly dimeric and having cysteine as a proximal heme ligand (Ghosh & Stuehr, 1995; Ghosh et al., 1996), but also differed in several ways. Specifically, its heme iron was six-coordinate low-spin, was able to bind a relatively bulky molecule like DTT, and upon reduction reacted with CO to form an unstable ferrous−carbon monoxide complex that converted over time to a cytochrome P420-like species. These properties are reminiscent of heme-containing iNOS monomers (Abu-Soud et al., 1995), which are also devoid of H4biopterin and contain a low-spin heme iron that binds DTT and forms an unstable ferrous−carbon monoxide complex.[4] This suggests that the heme environment in the H4biopterin-free dimer and monomer are similar regarding an increased solvent exposure, accommodation of larger ligands, and decreased stability relative to H4biopterin-replete iNOS dimer.

Spectral changes observed upon adding H4biopterin or L-arginine to the iNOSox dimer indicate that their binding was associated with gradual displacement of the DTT ligand and a shift toward five-coordinate high-spin heme. Thus, binding either molecule affects the heme in a similar way and appears to cause a conformational change that closes up the distal heme pocket. This is consistent with bound H4biopterin or L-arginine altering heme iron ligand access and binding geometry (Salerno et al., 1996; Matsuoka et al., 1994; Wang et al., 1994, 1995) and influencing covalent attachment of alkylating agents generated within the NOS active site (Gerber & Ortiz de Montellano, 1995). Although experimental data and mechanistic considerations strongly suggest that L-arginine affects the heme by binding directly above it in the distal heme pocket (Griffith & Stuehr, 1995; Marletta, 1993; McMillan & Masters, 1995; Matsuoka et al., 1994; Wang et al., 1994, 1995; Klatt et al., 1994a), it is presently unknown whether H4biopterin also does so, or instead affects the heme through a more global conformational change brought on by its binding at a distant site in the protein. In either case, we conclude from our present data that acquisition of dimeric structure alone does not detectably alter the heme environment in iNOSox, but it does enable H4biopterin and L-arginine to bind productively to the protein and cause changes consistent with a closing up of the distal heme pocket.

A unique feature of the H4biopterin-free iNOSox dimer is its susceptibility to trypsin proteolysis at residue K117. Because the proteolysis occurred under nondenaturing conditions, the protease was constrained to interact only with peptide regions that are exposed to solvent in an otherwise folded dimer. This implies that the region near K117 has dynamic elements and is exposed when the dimer is in a H4biopterin-free state. Indeed, when the protease specificity of the cleavage reaction was examined,[5] it was found to be susceptible only to Lys-C and resistant to proteases such as V8, Arg-C, or Asp-N, suggesting a primary role for K residue(s) in the cleavage reaction.

[4] H. M. Abu-Soud, D. K. Ghosh, and D. J. Stuehr, unpublished observation.

[5] D. K. Ghosh and D. J. Stuehr, unpublished observation.

H4biopterin was much more effective than L-arginine at protecting against proteolytic cleavage at K117. This contrasts with the similar effect these two molecules have on the iNOSox heme environment, and suggests that H4biopterin may function through a distinct additional mechanism. Protection could occur if bound H4biopterin directly blocks the cleavage site, or more likely, if its binding promotes or stabilizes a protein conformation that hides the susceptible basic residue(s) in the iNOSox dimer. The latter mechanism is analogous to bound substrate preventing proteolysis within a mobile region of cytochrome P-450_{2B1} (Tsokos et al., 1992). In the case of H4biopterin-free iNOSox, its N-terminal region appears relatively unfolded and exposed compared to the C-terminal two-thirds of the domain and thus may represent an intermediate structure on the pathway to fully folded native protein. An H4biopterin-induced conformational change in this region may be a means by which H4biopterin stabilizes iNOS dimeric structure (Abu-Soud et al., 1995; Ghosh et al., 1996; Baek et al., 1993). A model consistent with the current data that relates iNOSox prosthetic group binding to structural changes and catalytic function is presented in Figure 9.

Characterization of C109A iNOSox identified a residue located near K117 that influenced H4biopterin binding affinity but was otherwise not critical for dimeric interaction, catalysis, L-arginine binding, or heme pocket structure. C109A iNOSox required higher concentrations of H4biopterin to support NO synthesis, protect against proteolysis, and promote dimerization. This strongly suggests that all three effects depend on H4biopterin saturating a common binding site that is influenced by the C109 mutation. Our results are consistent with those of Chen et al. (1995), who showed mutation of the analogous C99 in full-length endothelial NOS decreased its H4biopterin binding affinity but did not alter L-arginine binding or catalytic properties.

Characterization of Δ117 iNOSox revealed that proteolytic removal of the N-terminal 117 residues destroyed the protein's capacity to maintain a dimeric structure and productively interact with H4biopterin or L-arginine. However, the proteolysis did not cause release of bound heme or alter its proximal thiolate ligand, indicating that the heme environment remained intact. Indeed, the mutant Δ114 iNOSox when expressed in bacteria had properties similar to proteolytically derived Δ117 iNOSox, confirming that the first 114 residues are important for dimeric structure and for productive H4biopterin and L-arginine interaction, but are not required for correct incorporation of heme into iNOSox.

The deletion mutant Δ65 iNOSox possessed properties that were identical to wild-type iNOSox, suggesting that the first 65 residues do not participate in aspects related to dimeric structure, substrate binding, and catalysis. This narrowed the region of importance down to residues 66−114. As shown in Figure 10, this 49 amino acid segment contains several sites where residues are identical or conserved among the NOS isoforms, starting in the mouse iNOS sequence at residue P76. Low homology prior to this point is consistent with the Δ65 deletion not affecting the properties of iNOSox. The overall sequence homology in the 49 residue region is only moderate, raising the possibility that its function could differ between the NOS isoforms.

Our current work identifies a 49 residue region located N-terminal from the heme-binding cysteine (C194) that is important regarding iNOS structure and function. This compliments studies that identified residues or regions in

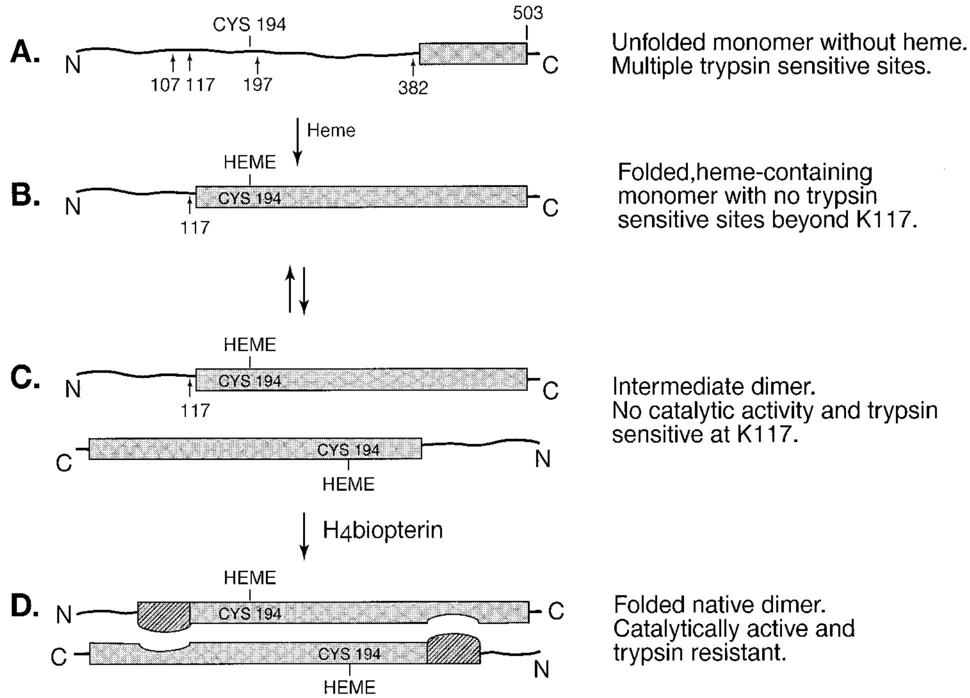

FIGURE 9: Model linking prosthetic group binding, structural change, and catalytic function of the iNOS oxygenase domain. In the absence of heme (A), the oxygenase domain is monomeric and has a relatively flexible structure as judged by its susceptibility to trypsin proteolysis at sites indicated by solid arrows throughout the domain. Incorporation of heme into the monomer (B) protects it from proteolysis beyond K117, suggesting heme incorporation stabilizes two-thirds of its structure. Simple dimerization of heme-containing monomers in the absence of H4biopterin (C) does not provide additional stabilization or change the heme environment. However, incorporation of H4biopterin into the dimer (D) stabilizes the N-terminal region against proteolysis, closes up the heme pocket, and activates the domain for NO synthesis. Thus, sequential incorporation of heme and H4biopterin cause a graded stabilization of the oxygenase domain.

```
Rat nNOS       274   VLNNPYSEDE   QPPTSGKKSP   TKNGSPSKCP   RFLKVKNWET   EVVLTDTLHL   323
Bovine eNOS     63   ----------   RPPEG-----   ---------P   KFPRVKNWEL   GSITYDTLCA    88
Mouse MacNOS    65   SLDKL-----   ----------   --HVTS-TRP   QYVRIKNWGS   GEILHDTLHH    96
Human iNOS      70   SLVKL-----   ----------   --DATPLSSP   RHVRIKNWGS   GMTFQDTLHH   102
Dros NOS       177   KMSQDY----   RSRAGSFMHL   DDEGRSLLMR   KPMRLKNIEG   RPEVYDTLHC   235
                                                        .    .  ..**  .      ***

Rat nNOS       324   KSTLETGCTE   YICMGSIMHP   SQ-H                                   346
Bovine eNOS     89   QSQQDGPCTP   RCCLGSLVLP   RKLQ                                   112
Mouse MacNOS    97   KATSDFTCKS   KSCLGSIMNP   KSLT                                   120
Human iNOS     103   KAKGILTCRS   KSCLGSIMTP   KSLT                                   123
Dros NOS       236   KGREILSCSK   ATCTSSIMN-   ---I                                   255
                     ..      *      * .*..
```

FIGURE 10: Amino acid sequence alignment between residues 65−120 of mouse iNOS and four related NOS isoforms. Residues (65−120) of mouse macrophage iNOS (Xie et al., 1992) are aligned with corresponding sequences of rat nNOS (Bredt et al., 1991), bovine eNOS (Sessa et al., 1992), human iNOS (Geller et al., 1993) and drosophila (Dros) NOS (Regulski & Tully, 1995). The asterisk (*) indicates a residue in the alignment that is completely conserved, while the dot (•) indicates that the residue is highly conserved. The alignment was done using PC/Gene software from Oxford Molecular Group.

the oxygenase domain located C-terminal from the heme-binding cysteine as important for dimeric interaction and possibly for L-arginine binding (Cho et al., 1995; Nishimura et al., 1995). The 49 residue region identified here is clearly essential for iNOS dimeric structure, because the rest of the oxygenase domain (∼386 residues) is incapable of forming or maintaining a stable dimer in its absence. However, the data we obtained with Δ114 and Δ117 iNOSox cannot on its own assign a role for this region in binding H4biopterin or L-arginine, because all monomeric forms of iNOS to date (including full-length wild-type iNOS monomer) have uniformly failed to bind these molecules as judged by spectral perturbation, radioligand binding, or direct incorporation assays (Abu-Soud et al., 1995; Baek et al., 1993; Klatt et al., 1996; Cho et al., 1995; Nishimura et al., 1995). Thus, any deletion (114, Δ117) or point mutation (G450A, A453I) that prevents iNOS dimer formation may also prevent detectable H4biopterin and L-arginine binding by default. In spite of this limitation, three additional observations reported here provide compelling evidence that the 49 amino acid region is involved in productive H4biopterin interaction. First, H4biopterin displayed a unique capacity to protect against proteolysis within this region at K117. Second, mutagenesis of a conserved residue within this region (C109A) altered H4biopterin binding affinity without affecting any other properties of the protein. Lastly, Δ114 iNOSox was judged completely unable to bind H4biopterin by several criteria even though it maintained a partial dimeric structure, indicating its dimeric form possessed a binding defect. How the 49 residue region identified here responds to H4biopterin or functions in controlling iNOS heme pocket structure and subunit interaction is unknown. However, our current results provide a clear foundation to investigate these possibilities.

ACKNOWLEDGMENT

Presented at the second meeting on the Biochemistry and Molecular Biology of Nitric Oxide, UCLA, CA, July, 1996. We thank Drs. R. Lyons and J. Cunningham for providing mouse iNOS cDNA, F. Dalquist for providing PCWori cDNA, P. Medberry and J. Parkinson for help in constructing the wild-type iNOSox expression vector, T. Slattery and C. Glaser for N-terminal amino acid sequencing, and J. Zhang and P. Clark for excellent technical assistance.

REFERENCES

Abu-Soud, H. M., Loftus, M., & Stuehr, D. J. (1995) *Biochemistry 34*, 11167−11175.
Baek, K. J., Thiel, B. A., Lucas, S., & Stuehr, D. J. (1993) *J. Biol. Chem. 268*, 21120−21129.
Betton, J.-M., Desmadril, M., Yon, J. M. (1989) *Biochemistry 28*, 5421−5428.
Bredt, D. S., & Snyder, S. H. (1994) *Annu. Rev. Biochem. 63*, 175−195.
Bredt, D. S., Hwang, P. M., Glatt, C. E., Lowenstein, C., Reed, R. R., & Snyder, S. H. (1991) *Nature 351*, 714−718.
Brunner, F., & Kukovetz, W. R. (1991) *Br. J. Pharmacol. 102*, 373−380.
Caroll, L. J., Xu, Y. Thrall, S. H., Martin, B. M., & Dunaway-Mariano, D. (1994) *Biochemistry 33*, 1134−1142.
Chen, P.-F., Tsai, A.-L., & Wu, K. K. (1994) *J. Biol. Chem. 269*, 25062−25066.
Chen, P.-F., Tsai, A. L., & Wu, K. K. (1995) *Biochem. Biophys. Res. Commun. 215*, 1119−1129.
Chen, P.-F., Tsai, A.-L., Berka, V., & Wu, K. K. (1996) *J. Biol. Chem. 271*, 14631−14635.
Cho, H. J., Xie, Q.-w., Calaycay, J., Mumford, R. A., Swiderek, K. M., Lee, T. D., & Nathan, C. (1992) *J. Exp. Med. 176*, 599−604.
Cho, H. J., Martin, E., Xie, Q.-w., Sassa, S., & Nathan, C. (1995) *Proc. Natl. Acad. Sci. 92*, 11514−11518.
Fossetta, J. D., Niu, X. D., Lunn, C. A., Zavodny, P. J., Narula, S. K., Lundell, D. (1996) *FEBS Lett. 379*, 135−138.
Geller, D. A., Lowenstein, C. J., Shapiro, R. A., Nussler, A. K., DiSilvio, M., Wang, S. C., Nakayama, D. K., Simmons, R. L., Snyder, S. H., & Billiar, T. R. (1993) *Proc. Natl. Acad. Sci. U.S.A. 90*, 3491−3495.
Gerber, N. C., & Ortiz de Montellano, P. R. (1995) *J. Biol. Chem. 270*, 17791−17796.
Ghosh, D. K., & Stuehr, D. J. (1995) *Biochemistry 34*, 801−807.
Ghosh, D. K., Abu-Soud, H. M., & Stuehr, D. J. (1995) *Biochemistry 34*, 11316−11320.
Ghosh, D. K., Abu-Soud, H. M., & Stuehr, D. J. (1996) *Biochemistry 35*, 1444−1449.
Gibbs, A. F., Chapman, D., & Baldwin, S. A. (1988) *Biochem. J. 256*, 421−428.
Griffith, O. W., & Stuehr, D. J. (1995) *Annu. Rev. Physiol. 57*, 707−736.
Gross, S. S., & Levi, R. (1992) *J. Biol. Chem. 267*, 25722−25729.
Inaba, K., & Mohri, H. (1989) *J. Biol. Chem. 264*, 8384−8388.
Klatt, P., Schmidt, K., Brunner, F., & Mayer, B. (1994a) *J. Biol. Chem. 269*, 1674−1680.
Klatt, P., Schmid, M., Leopold, E., Schmidt, K., Werner, E. R., & Mayer, B. (1994b) *J. Biol. Chem. 269*, 13861−13866.
Klatt, P., Schmidt, K., Lehner, D., Glatter, D., Bachinger, H. P., & Mayer, B. (1995) *EMBO J. 14*, 3687−3695.
Klatt, P., Pleiffer, S., List, M. B., Lehner, D., Glatter, O., Bachinger, H. P., Werner, E. R., Schmidt, K., Mayer, B. (1996) *J. Biol. Chem. 271*, 7336−7342.
Kroncke, K. D., Fehsel, K., & Kolb-Bachofen, V. (1995) *Biol. Chem. Hoppe-Seyler 376*, 327−343.
Liu, B., Meloche, S., McNicoll, N., Lord, C., & Delean, A. (1989) *Biochemistry 28*, 3599−3605.
Marletta, M. A. (1993) *J. Biol. Chem. 268*, 12231−12234.
Martasek, P., Liu, Q., Roman, L. J., Gross, S. S., Sessa, W. C., & Masters, B. S. S. (1996) *Biochem. Biophys. Res. Commun. 219*, 359−365.
Matsuoka, A., Stuehr, D. J., Olson, J. S., Clark, P., & Ikeda-Saito, M. (1994) *J. Biol. Chem. 269*, 20335−20339.
McMillan, K., & Masters, B. S. S. (1993) *Biochemistry 32*, 9875−9890.
McMillan, K., & Masters, B. S. S. (1995) *Biochemistry 34*, 3586−3693.
Moncada, S., Palmer, R. M., & Higgs, E. A. (1991) *Pharmacol. Rev. 43* 109−142.
Nathan, C., & Xie, Q.-w. (1994) *Cell 79*, 915−918.
Nishimura, J. S., Martasek, P., McMillan, K., Salerno, J. C., Liu, Q., Gross, S. S., & Masters, B. S. S. (1995) *Biochem. Biophys. Res. Commun. 210*, 288−294.
Pufahl, R. A., Wishnok, J. S. , & Marletta, M. A. (1995) *Biochemistry 34*, 1930−1941.
Regulski, M., & Tully, T. (1995) *Proc. Natl. Acad. Sci. U.S.A. 92*, 9072−9076.
Renaud, J. P., Boucher, J. L., Vadon, S., Delaforge, M., & Mansuy, D. (1993) *Biochem. Biophys. Res. Commun. 192*, 53−60.
Richards, M. K., & Marletta, M. A. (1994) *Biochemistry 33*, 14723−14732.
Rodriguez-Crespo, I., Counts-Gerber, N., & Ortiz de Montellano, P. R. (1996) *J. Biol. Chem. 271*, 11462−11467.
Roman, L. J., Sheta, E. A., Martasek, P., Gross, S. S., Liu, Q., & Masters, B. S. S. (1995) *Proc. Natl. Acad. Sci. U.S.A. 92*, 8428−8432.
Salerno, J. C., Martasek, P., Roman, L. J., & Masters, B. S. S. (1996) *Biochemistry 35*, 7626−7630.
Sari, M.-A., Booker, S., Jaouen, M., Vadon, S., Boucher, J.-L., Pompon, D., & Mansuy, D. (1996) *Biochemistry 35*, 7204−7213.
Sessa, W. C., Harrison, J. K., Barber, C. M., Zeng, D., Durieux, M., D'Angelo, D. D., Lynch, K. R., & Peach, M. J. (1992) *J. Biol. Chem. 267*, 15274−15276.
Sheta, E. A., McMillan, K., & Masters, B. S. S. (1994) *J. Biol. Chem. 269*, 15147−15153.
Siddhanta, U., Wu, C., Abu-soud, H. M., Zhang, I., Ghosh, D. K., & Stuehr, D. J. (1996) *J. Biol. Chem. 271*, 7309−7312.
Sono, M., Anderson, L. A., & Dawson, J. H. (1982) *J. Biol. Chem. 257, 8308*−8320.
Stuehr, D. J., & Ikeda-Saito, M. (1992) *J. Biol. Chem. 267*, 20547−20550.
Tsokos, D. C., Omata, Y., Robinson, R. C., Krutzsch, H. C., Gelboin, H. V., & Friedman, F. K. (1992) *Biochemistry 31*, 7155−7159.
Tzeng, E., Billiar, T. R., Robbins, P. D., Loftus, M., & Stuehr, D. J. (1995) *Proc. Natl. Acad. Sci. U.S.A. 92*, 11771−11775.
Wang, J., Rousseau, D. L., Abu-Soud, H. M., & Stuehr, D. J. (1994) *Proc. Natl. Acad. Sci. U.S.A. 91*, 10512−10516.
Wang, J., Stuehr, D. J., & Rousseau, D. L. (1995) *Biochemistry 34*, 7080−7087.
Wu, C., Zhang, J., Abu-Soud, H. M., Ghosh, D. K., & Stuehr, D. J. (1996) *Biochem. Biophys. Res. Commun. 222*, 439−444.
Xie, Q.-w., Cho, H. J., Calaycay, J., Mumford, R. A., Swiderek, K. M., Lee, T. D., Ding, A., Troso,T., & Nathan, C. (1992) *Science 256*, 225−228.
Xie, Q-w., Leung, M., Fuortes, M., Sassa, S., & Nathan, C. (1996) *Proc. Natl. Acad. Sci. U.S.A. 93*, 4891−4896.

BI9702290